BMC Genomics

RESEARCH Open Access

Integrated transcriptome and metabolism unravel critical roles of carbon metabolism and oxidoreductase in mushroom with Korshinsk peashrub substrates

Yuan Zhao[1,2*], Youhua Yao[1,3,4,5], Hongying Li[1,2], Zirui Han[1,2] and Xuewen Ma[1,2]

Abstract

Edible fungi cultivation serves as an efficient biological approach to transforming agroforestry byproducts, particularly Korshinsk peashrub (KP) branches into valuable mushroom (*Lentinus edodes*) products. Despite the widespread use of KP, the molecular mechanisms underlying its regulation of mushroom development remain largely unknown. In this study, we conducted a combined analysis of transcriptome and metabolism of mushroom fruiting bodies cultivated on KP substrates compared to those on apple wood sawdust (AWS) substrate. Our aim was to identify key metabolic pathways and genes that respond to the effects of KP substrates on mushrooms. The results revealed that KP induced at least a 1.5-fold increase in protein and fat content relative to AWS, with 15% increase in polysaccharide and total sugar content in mushroom fruiting bodies. There are 1196 differentially expressed genes (DEGs) between mushrooms treated with KP relative to AWS. Bioinformatic analysis show significant enrichments in amino acid metabolic process, oxidase activity, malic enzyme activity and carbon metabolism among the 698 up-regulated DEGs induced by KP against AWS. Additionally, pathways associated with organic acid transport and methane metabolism were significantly enriched among the 498 down-regulated DEGs. Metabolomic analysis identified 439 differentially abundant metabolites (DAMs) in mushrooms treated with KP compared to AWS. Consistent with the transcriptome data, KEGG analysis on metabolomic dataset suggested significant enrichments in carbon metabolism, alanine, aspartate and glutamate metabolism among the up-regulated DAMs by KP. In particular, some DAMs were enhanced by 1.5-fold, including D-glutamine, L-glutamate, glucose and pyruvate in mushroom samples treated with KP relative to AWS. Targeted metabolomic analysis confirmed the contents of DAMs related to glutamate metabolism and energy metabolism. In conclusion, our findings suggest that reprogrammed carbon metabolism and oxidoreductase pathways act critical roles in the enhanced response of mushroom to KP substrates.

Keywords Korshinsk peashrub branches, *Lentinula edodes*, Transcriptome, Metabolism, Carbon metabolism, Amino acids biosynthesis

*Correspondence:
Yuan Zhao
2011990023@qhu.edu.cn

Full list of author information is available at the end of the article

Introduction

Korshinsk peashrub (*Caragana korshinskii* Kom.), a resilient and drought-tolerant perennial mesquite shrub is widely distributed in northeastern, northwestern and northern regions of China [1, 2]. The adaptability and high survival rate of Korshinsk peashrub (KP), coupled with its robust resistance to cold, drought and barren lands have led to its widespread planting on the Loess Plateau and in desert regions. This strategic planting aims to combat soil erosion and facilitate vegetation restoration [3, 4]. Notably, KP exhibits exceptional branching and regenerative capabilities, necessitating regular pruning every four to five years. The annual yield of KP branches is estimated to be around 550,000 tons, representing a substantial lignocellulosic biomass resource [5–7]. Currently, KP finds applications as fodder, fuel energy and plant fertilizer; however, these uses only exploit a fraction of its potential. Unfortunately, a significant portion of chopped KP is discarded or released directly into the land and rivers, resulting in environmental pollution and resource wastage. Addressing this challenge is now a pivotal concern for policymakers and scientists alike, prompting the exploration of novel strategies to maximize the utilization of KP biomass.

Cultivating edible fungi has proven to be an efficient biological method for transforming agroforestry byproducts into valuable mushroom products, establishing a direct connection between lignocellulosic waste and human food consumption [8, 9]. Numerous studies have explored the pivotal role of KP as a substrate ingredient for cultivating various *Pleurotus*. spp., including *Pleurotus eryngii*, *Pleurotus ostreatus* and *Pleurotus tuoliensis* [10–12]. Utilizing KP as a substrate for *Pleurotus*. spp. production not only ensures the efficient utilization of lignocellulosic waste but also addresses the shortage of conventional raw materials, such as cottonseed hull. Despite the potential benefits, the process of fruiting body development in mushrooms is very complex. Mushroom fruiting is subject to regulation by a range of cellular processes, genetic factors, physiological aspects and environmental influences, all playing crucial roles in normal fruiting [13]. However, the molecular mechanisms through which KP regulates mushroom development remain largely unknown.

In recent years, mass spectrometry (MS)-based metabolomics approaches have gained widespread use for studying metabolite profiles that indicate key biosynthetic pathways governing the temporal growth and development of plants [14, 15]. However, only a limited number of metabolomics studies have reported on the metabolic disparity among mushrooms across spatial dimensions and cultivars [16]. The integration of metabolomics and transcriptomics represents a powerful approach for understanding the intertwined metabolism and molecular mechanisms of gene regulation by constructing a unified pathway [17–19]. Indeed, numerous studies have examined various microbes and plants such as *Arabidopsis*, *Salvia* and *Penicillium* species using an integrated metabolomics–transcriptomics approach to reveal mechanisms underlying the biosynthesis of functional bio-actives including flavonoids, polyketides and terpenoids [17–19]. However, omics analyses of *L. edodes* have primarily focused on the developmental process from mycelium to fruiting bodies [20, 21], with few reports on integrated transcriptomics and metabolomics analyses concerning malformed *L. edodes* fruiting bodies.

In this study, we conducted a comprehensive analysis by integrating transcriptome and metabolomics assessments of mushroom fruiting bodies cultivated on KP substrates and apple wood sawdust (AWS) substrates. The aim was to furnish preliminary data, deciphering key metabolic pathways and genes responsive to the distinct effects of substrates in mushrooms. Additionally, qPCR and targeted metabolomics were employed to validate changes in key genes or metabolites within the mushroom samples with KP and AWS substrates. The identification of key regulatory factors for mushrooms with KP substrates will help to guide precise gene editing strategies, ultimately enhancing the economic benefits of mushroom production.

Materials and methods

Materials and growth conditions

In this study, we focus on the L808 mushroom variety which is extensively cultivated in Northwest China. The experiment was conducted from January to December 2019 at the Shiitake Mushroom Production Base in Menyuan County, Qinghai Province (37°39′N, 101°63′E, altitude 3700 m). The region has a plateau continental climate with annual precipitation of 530–560 mm and an average annual temperature of 1.3 °C.

Two different fruit tree cultivation substrates, namely Korshinsk peashrub branch (KP) and apple wood sawdust (AWS) were employed. Alternative names for KP and AWS are Caragana korshinskii and Malus Pumila Mill, respectively. Both substrates as local common mushroom substrates were purchased from Qinghai Huagu Mushroom Industry Technology Co., Ltd. Accordingly, two cultivation formulas were configured (KP group: 78% KP, 20% bran, 1% gypsum powder, 1% sucrose; AWS group: 78% apple wood, 20% bran, 1% gypsum powder, sucrose 1%). Standard methods for fruiting management were followed [22]. From each wood substrate group, 10 mushroom fruiting bodies were randomly selected based on relatively consistent maturity, absence of mechanical damage, closed caps (no umbrella opening), no sign of disease and uniform size. The base cultivation substrates were removed, cut into 3 mm slices, mixed into

one replicate and a total of 6 replicates were obtained resulting in 12 samples that were promptly frozen in liquid nitrogen.

Nutritional trait measurements

Free fatty acids, crude protein and total dietary fiber contents were determined following the method outlined by the Association of Analytical Chemists [23] with slight modification [24]. The polysaccharides of mushroom fruiting bodies were extracted according to a previously reported method with minor adjustments [25]. Briefly, 2 g of fruiting body powder was subjected to extraction with 80 ml of 80% ethanol at 90 °C for 60 min to eliminate pigments, small sugar molecules and impurities. Insoluble residues were dried and then subjected to two additional extractions with 80 ml of distilled water at 90 °C for 1 h each. The extracts were filtered and the filtrate was obtained after centrifugation at 4500×g for 15 min. Total sugar content was determined calorimetrically using anthrone reagent based on the method of McCready [26].

mRNA extraction and transcriptome sequencing

Total RNA extraction was carried out using Trizol Reagent (Thermo Fisher, Carlsbad, CA, USA) in accordance with the manufacturer's instructions. The NanoDrop spectrophotometer was utilized for determining RNA concentration. To monitor RNA degradation and contamination, 1% agarose gels were employed and purity was checked using the Nano-Photometer spectrophotometer (IMPLEN, Carlsbad, CA, USA). The integrity of RNA was assessed using the RNA Nano 6000 Assay Kit of the Agilent Bioanalyzer 2100 system (Agilent Technologies, CA, USA). For RNA sample preparations, 1.5 μg of RNA per sample was used as input material. Sequencing libraries were generated with the NEB Next Ultra RNA Library Prep Kit for Illumina (NEB, Carlsbad, CA, USA), following the manufacturer's recommendations. Index codes were added to attribute sequences to each sample. Index-coded sample clustering was performed on a Bot Cluster Generation System using the HiSeq 4000 PE Cluster Kit (Illumina, USA) [27]. Subsequently, library preparations were sequenced on an Illumina Hiseq 4000 platform generating 150-bp paired-end reads [28].

The quality of RNA-seq data (fastq files) was assessed using FastQC software (http://www.bioinformatics.babraham.ac.uk/projects/fastqc/). Adapters and reads with low quality from raw RNA-seq reads were trimmed using trim_galore software (http://www.bioinformatics.babraham.ac.uk/projects/trim_galore/; adaptor of read1: AGATCGGAAGAGCACACGTCTGAACTCCAGTCAC; adaptor of read2: AGATCGGAAGAGCGTCGTGTAGGGAAAGAGTGT). RNA-seq analysis was performed by the STAR software (version 2.5.3a; http://github.com/alexdobin/STAR; accessed on 13th Apr 2021) [29] with the *Pleurotus*. Spp. reference genome (https://www.ncbi.nlm.nih.gov/data-hub/taxonomy/213554/; accessed on 18th Jul 2021). Fragments per kilobase of transcript per million mapped reads (FPKM) values were calculated using cufflinks software (v2.2.1, http://cole-trapnell-lab.github.io/cufflinks/; accessed on 10th May 2021) to compare the relative abundance of genes in mushroom fruiting bodies by KP and AWS.

Differentially expressed gene (DEG) analysis in mushroom fruiting bodies by KP and AWS adhered to specific criteria. A DEG was considered as a gene with a fold-change (FC) ≥ 2 or FC ≤ 0.5, representing the upregulated and downregulated DEGs, respectively, with an adjusted $p < 0.05$. Volcano plots were generated to visually represent DEGs in transcriptome analyses.

GO functional and KEGG pathway enrichments

Gene Ontology (GO) functional enrichment and Kyoto Encyclopedia of Genes and Genomes (KEGG) pathway enrichment were analyzed based on the list of DEGs identified in mushroom fruiting bodies by KP and AWS. The pathway ID's enrichment *p*-value was calculated using Fisher's exact test. Terms meeting the criteria of a *p*-value < 0.05 and gene counts ≥ 2 were selected as differential terms. The most significant GO and KEGG terms were visually represented through column charts.

Verification of DEGs by qPCR

The ten common DEGs in mushroom fruiting bodies by KP and AWS were validated using real-time qPCR with primer details listed in Table S1. Total RNA was extracted using the TrizolTM Reagent (Thermo Fisher, Carlsbad, CA, USA) following the manufacturer's instructions. RNA concentration was determined using the NanoDrop spectrophotometer. Subsequent to reverse transcription with the PrimeScript RT Master Mix (Perfect Real Time, Takara, Shanghai, China) and the microRNA RT-PCR system (BioTNT, A2030A001-120T, Hangzhou, China), cDNA was obtained and stored at −20 °C [30]. The qPCR reaction volume included 10 μL UNICONTM qPCR SYBR Green Master Mix, 1 μL of the primer mixture (200 nM), 6 μL of cDNA templates and 6 μL of RNase-free ddH2O. The thermocycler program was as follows: 3 min at 95 °C; 40 cycles of 10 s at 95 °C and 20 s at 65 °C; 30 s at 72 °C, 1 min at 65 °C and 15 s at 95 °C. Relative mRNA expression levels were calculated using the comparative $2^{-\Delta\Delta Ct}$ method with 16 S rRNA as the reference gene. The significant difference for the expression level of each gene was determined based on Student *t*-test. All reactions were performed in triplicate to ensure experimental reproducibility and reliability of the results.

Metabolism determinations

Non-targeted metabolic profiling in mushroom fruiting bodies by KP and AWS was conducted using the LC-MS/MS with Triple Quad 6500 SCIEX [31]. Approximately 2.5 mg of mushroom fruiting bodies were sampled in 2 ml Eppendorf tube containing pre-cooled metal beads and immediately stored in liquid nitrogen. The samples were initially extracted using a ball mill at 30 Hz for 5 min. The extracted powder was then dissolved in 1.5 ml methanol/chloroform mixture and incubated at −20 °C for 5 h. Subsequently, the mixture was centrifuged at 2000 g and 4 °C for 10 min and filtered using 0.43 μm organic phase medium (GE Healthcare, 6789–0404).

Metabolomic analysis was performed using metabolon software (Durham, NC, USA). The sample components were identified by comparing the retention time and mass spectra with those of the reference metabolites. For metabolic compound identification in each sample, it is highly recommended to reference the mass spectra with entries from the NIST02 and Golm metabolome database (http://csbdb.mpimp-golm.mpg.de/csbdb/gmd/gmd.html). The differential abundant metabolites (DAMs) were determined according to their peak signal intensities based on Student *t*-test.

Energy metabolism determinations

To elucidate the changes in metabolites involved in the energy metabolic pathway, a targeted-metabolism analysis was conducted [32]. Mushroom fruiting bodies were extracted in 2 mL Eppendorf (Ep) tubes filled with pre-cooled metal beads and immediately stored in liquid nitrogen. The samples underwent extraction with a ball mill at 30 Hz for 3 min. The extracting powder was dissolved in 1.3 mL methanol/chloroform and incubated at −20 °C for 4 h. Subsequently, the mixture was centrifuged at 2000 g at 4 °C for 10 min followed by filtration with a 0.43 μm organic phase medium (GE Healthcare, 6789−0404). A 200 μL was added to the HPLC sample bottle with a lined tube and store at −80 °C until use. Metabolites related to the energy metabolic pathway, each with independent standard curves were determined using LC-MS/MS (AB Sciex Qtrap 6500; SCIEX). The column used was a 100×2 mm Phenomenex Luna 3 μm NH_2 (Catalog No.: 00D-4377-B0, 0.314 mL volume). The detection wavelength was set at 190 nm and the injection volume was 20 μL with a column temperature of 20 °C and a flow speed of 0.4 mL/min. The mobile phase comprised 15% buffer A (95% H_2O and 5% ACN, pH = 9.5) + 85% buffer B (100% ACN) at a rate of 0.2 mL/min. Five biological replicates were conducted for metabolic measurements and the linear regression index for the standard curve ranged between 0.88 and 0.99. Differentially accumulated metabolites were determined by limma package in R. The significance of difference for each identified metabolite was determined based on Student *t*-test in the mushroom samples between KP and AWS.

Results

In this study, we analyzed the effect of two wood sawdust substrates (KP and AWS) on the development of the mushroom (*Lentinula edodes*). We observed that mushrooms treated with KP substrates exhibited a darker body color compared to those treated with AWS substrates (Fig. 1A). Relative to AWS, KP treatment resulted in at least a 1.5-fold increase in crude protein and fatty acid contents though crude fiber content remained unchanged (Fig. 1B-D). Accordingly, KP treatment led to 60% increase in crude fat content in mushroom fruiting bodies without significant changes in crude protein and fiber content (Fig. 1E-G).

Our findings also revealed that polysaccharide and total sugar contents were at least 15% higher in KP-treated mushroom samples compared to those treated with AWS (Figures S1A-B). To identify differentially expressed genes (DEGs) between AWS and KP treatments, we conducted a combined transcriptome and metabolism analysis. Principal component analysis (PCA) of the transcriptome dataset revealed that PC1 and PC2 accounted for 63% and 14% of the variance, respectively, in samples treated with AWS and KP (Fig. 2A). The average number of raw reads across 12 mushroom samples treated with AWS and KP was 46.4 million with clean reads comprising 99.2% of total raw reads (Table S2). The Q20 and Q30 values were 97% and 93%, respectively (Table S2). We identified 1196 DEGs including 698 upregulated and 498 down-regulated genes (Fig. 2B), with the top 10% DEGs for downregulation and upregulation were listed in Table S3 and S4, respectively. These DEGs were visualized in Fig. 2C. Transcriptome analysis revealed that read error rates ranged from 0.02 to 0.03 within the 300-bp reads for mushrooms treated with both AWS and KP substrates (Figures S2A-B). Regarding base content, the contents of the four bases (A, T, C and G) each accounted for approximately 25% of total reads within 300-bp range for mushroom samples under both AWS and KP treatments (Figures S3A-B).

GO enrichment analysis highlighted significant enrichment of pathways related to D-amino acid metabolic process, oxidase activity, ion binding, FAD binding, malic enzyme activity, malate dehydrogenase activity and flavin adenine dinucleotide binding in the upregulated DEGs in KP-treated mushroom samples compared to AWS-treated ones (Fig. 3A). Conversely, pathways associated with amino acid transmembrane transport, organic acid transport and oxidoreductase activity were significantly enriched in downregulated DEGs in KP-treated samples relative to AWS-treated ones (Fig. 3B).

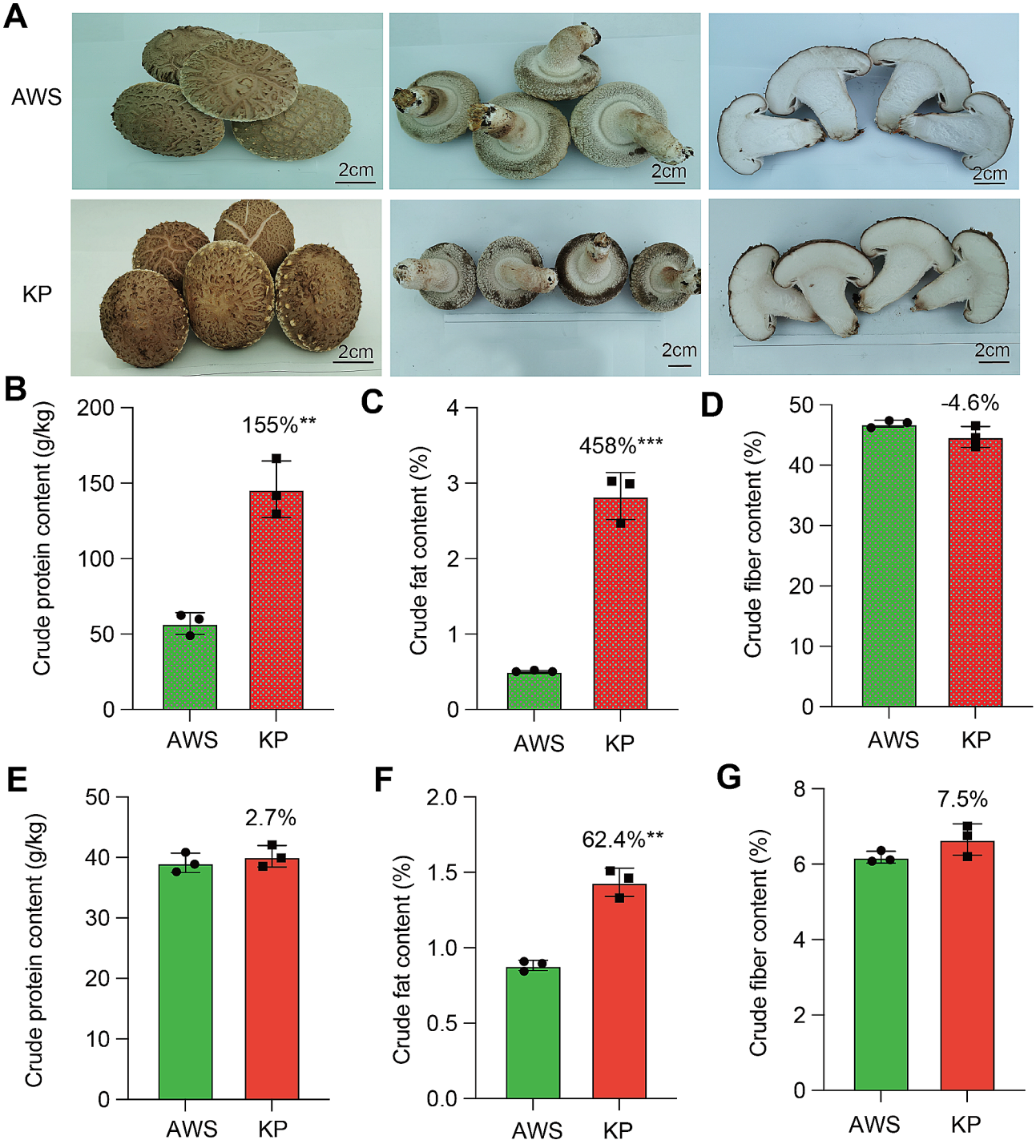

Fig. 1 Effects of two wood sawdust substrates on the development of *Lentinula edodes* mushroom. **A**, Images of *Lentinula edodes* mushrooms treated with two wood sawdust substrates: KP (Korshinsk peashrub) and AWS (apple wood sawdust). Scale bar for each image is proportional to 2 cm. **B**-**D**, Crude protein content, crude fat content and crude fiber content for AWS and KP substrates. **E**-**G**, Crude protein content, crude fat content and crude fiber content for *Lentinula edodes* bodies treated with AWS and KP substrates. Data represent means ± S.E. ($n = 3$). Numbers represent percentage differences in KP relative to AWS. Symbols "**" and "***" represent significant differences at $P < 0.01$ and $P < 0.001$, respectively, based on Student *t*-test

KEGG analysis further revealed significant enrichment in the biosynthesis of secondary metabolites, biosynthesis of amino acids, carbon metabolism, oxidative phosphorylation, pyruvate metabolism, glycine, serine and threonine metabolism in upregulated DEGs in KP-treated mushroom samples compared to AWS-treated ones (Fig. 4A). In contrast, microbial metabolism in diverse environments, sphingolipid signaling pathway,

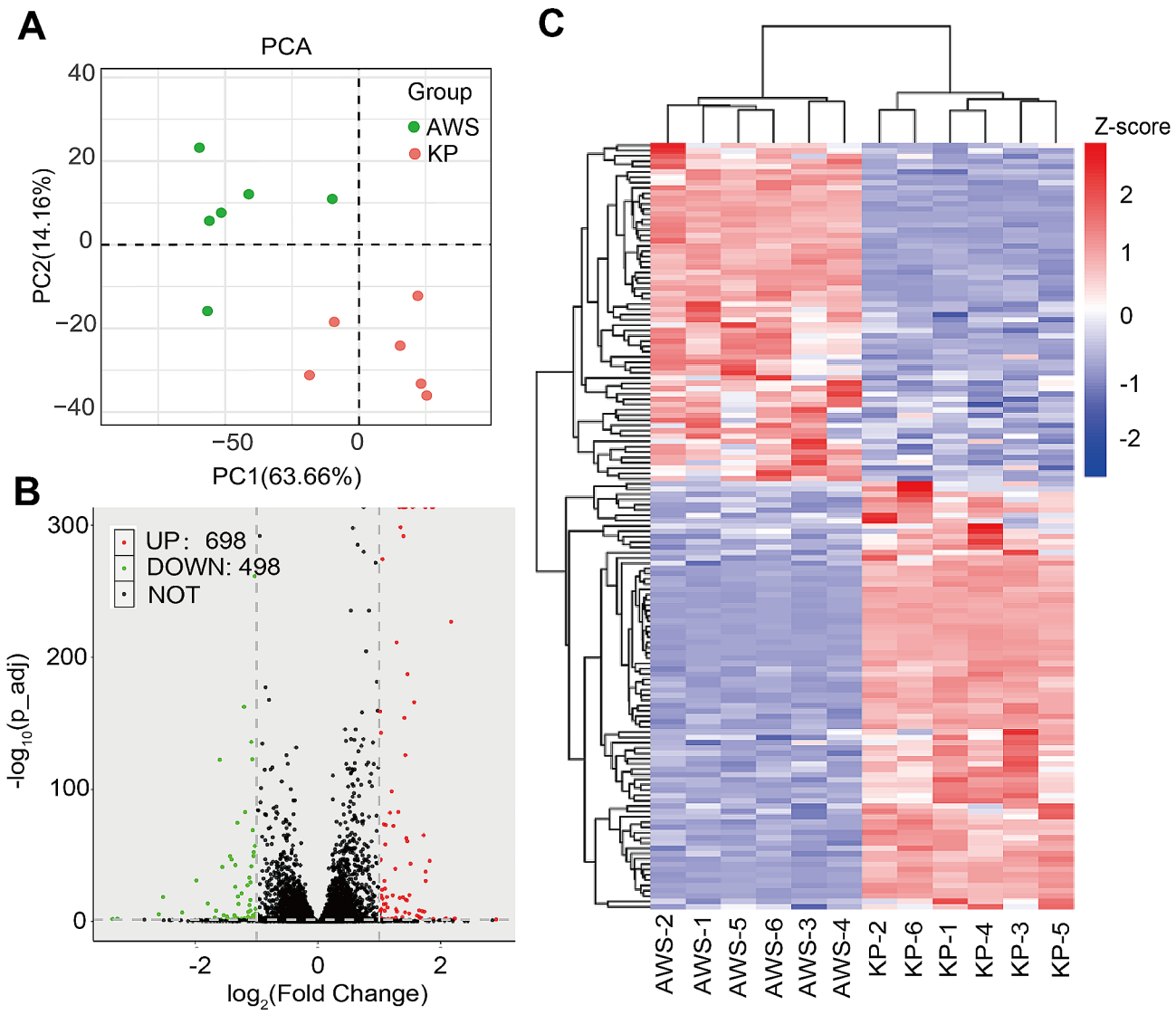

Fig. 2 Differentially expressed genes (DEGs) in *Lentinula edodes* mushrooms treated with two wood sawdust substrates. **A**, Principal component analysis on transcriptome. **B**, Volcano plot representing the DEGs between AWS and KP in *Lentinula edodes*. **C**, heatmap representing the DEGs in different samples of *Lentinula edodes* treated with two wood sawdust substrates (KP and AWS)

estrogen signaling pathway, glyoxylate and dicarboxylate metabolism pathway, and methane metabolism pathways were significantly enriched in downregulated DEGs in KP-treated samples relative to AWS-treated ones (Fig. 4B).

To identify key DEGs involved in the distinct regulation between the two substrates (KP and AWS) in mushroom samples, we performed qPCR experiments on the top 1% DEGs, identifying five upregulated and five downregulated DEGs induced by KP relative to AWS (Fig. 5A). The patterns of these downregulated DEGs including *LENED_008220*, *LENED_007446*, *LENED_001270*, *LENED_001907 and LENED_002235* closely matched those observed in the transcriptome analysis (Fig. 5B-F). Conversely, the relative expression levels of all five upregulated DEGs were slightly or significantly increased in mushroom samples induced by KP relative to AWS (Fig. 5G-K).

To further elucidate the altered metabolic pathways in response to KP relative to AWS treatments in mushroom samples, we conducted non-targeted metabolism analysis targeted metabolite analysis related to the energy metabolic pathway. PCA indicated clear separation between samples within each group (either AWS or KP) highlighting the effectiveness of substrate treatment in mushroom samples (Fig. 6A). We identified 275 upregulated and 164 downregulated differentially abundant metabolites (DAMs) in KP-induced mushroom samples compared to AWS-induced ones (Fig. 6B; Table S5). KEGG analysis of DAMs revealed significant enrichment in the mTOR

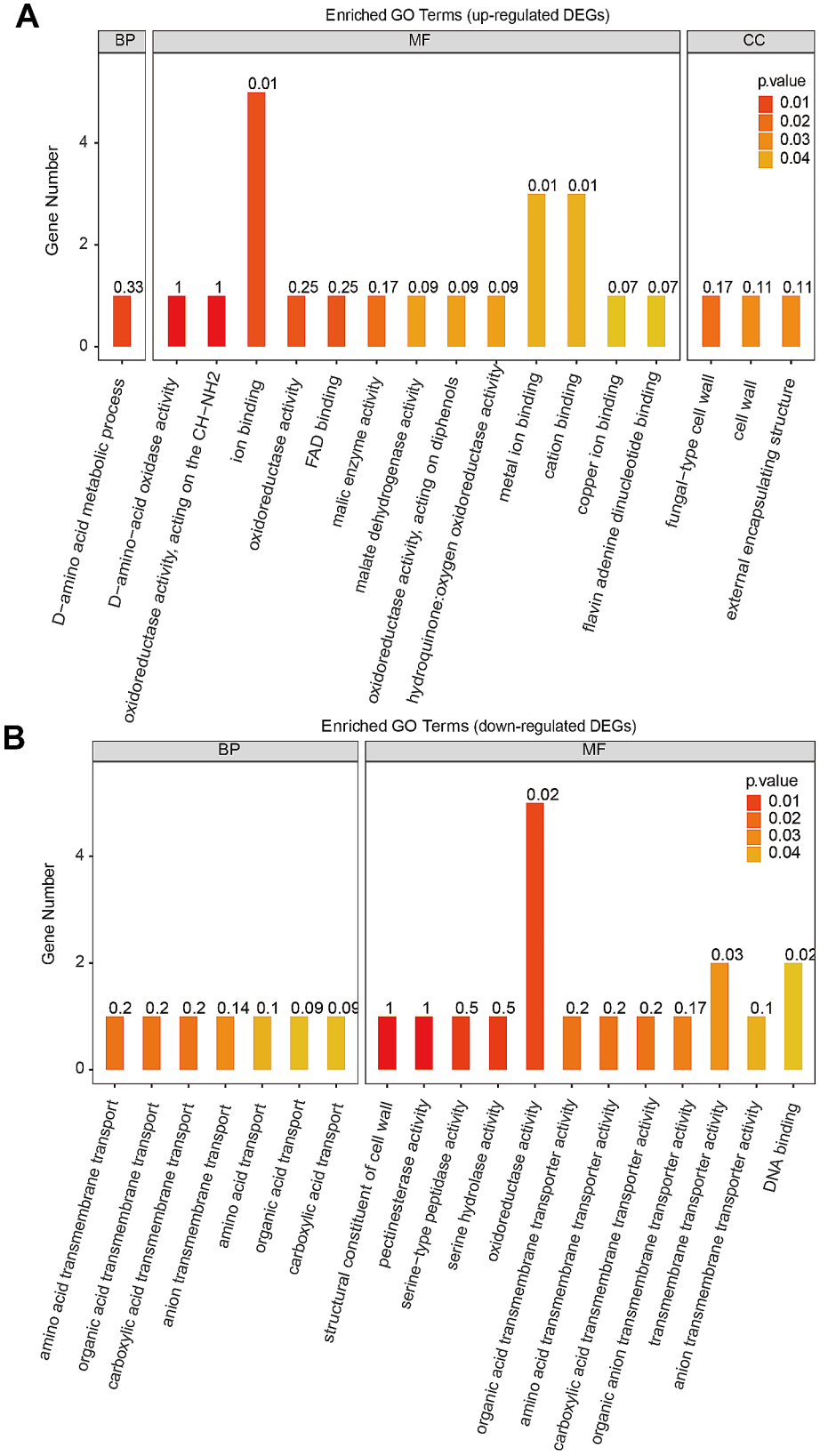

Fig. 3 Gene Ontology (GO) enrichment analysis on differentially expressed genes in *Lentinula edodes* with two wood sawdust substrates treatments. **A**, GO analysis on the up-regulated DEGs induced by KP relative to AWS. **B**, GO analysis on the down-regulated DEGs induced by KP relative to AWS

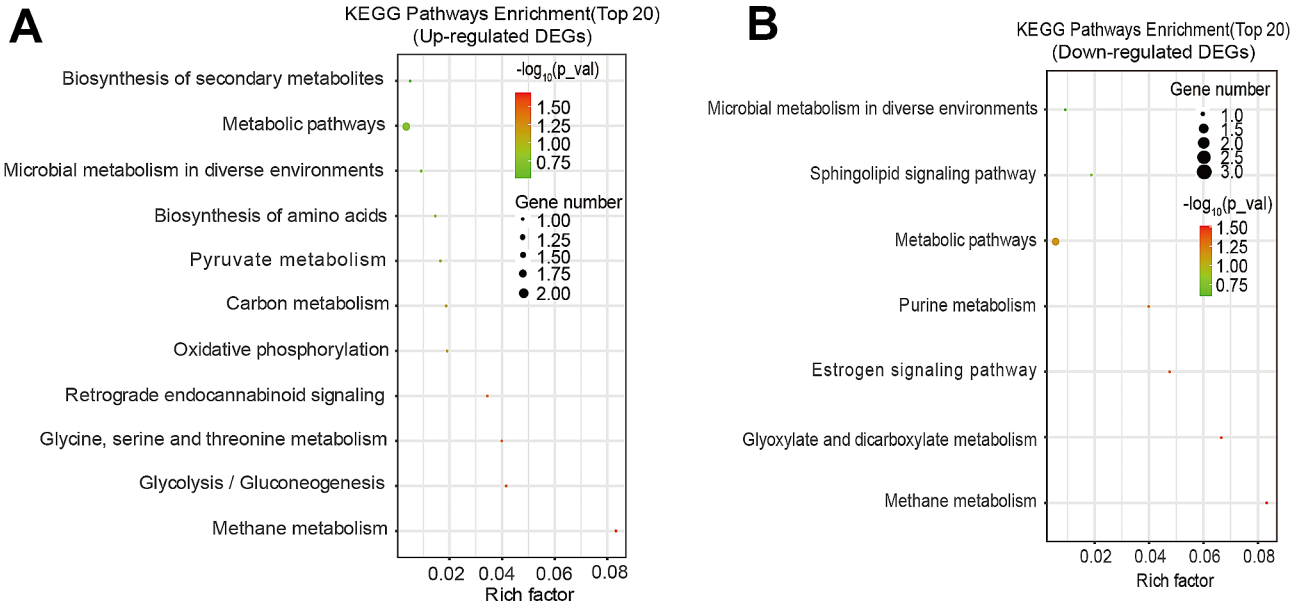

Fig. 4 Kyoto Encyclopedia of Genes and Genomes (KEGG) analysis on the differentially expressed genes in *Lentinula edodes* with two wood sawdust substrates treatments. **A**, KEGG analysis on up-regulated DEGs induced by KP relative to AWS. **B**, KEGG analysis on down-regulated DEGs induced by KP relative to AWS

signaling pathway, central carbon metabolism, arginine biosynthesis, alanine, aspartate and glutamate metabolism, biosynthesis of amino acids, and fructose and mannose metabolism pathways between AWS and KP treatments (Fig. 6C).

Pathway hierarchy enrichment analysis indicated significant enrichment in pathways related to proximal tubule bicarbonate reclamation, D-glutamine and D- glutamate metabolism, glycolysis/gluconeogenesis, pentose phosphate pathway, carbon metabolism, alanine, aspartate and glutamate metabolism, fructose and mannose metabolism, amino sugar and nucleotide sugar metabolism, and biosynthesis of amino acids among upregulated DAMs (Fig. 7A). Conversely, mineral absorption, D-arginine and D-ornithine metabolism, and mTOR signaling pathways were significantly enriched among downregulated DAMs in AWS-treated mushroom samples compared to KP-treated ones (Fig. 7A). Notably, most organic acids and derivatives, organic oxygen compounds, and nucleosides and analogues were upregulated by KP relative to AWS, except for ethylene glycol dodecyl ether sulfate (Fig. 7B). However, most metabolites related to lipids and lipid-like molecules were downregulated in KP-treated mushroom samples compared to AWS-treated ones (Fig. 7B).

Integrative analysis of transcriptome and metabolism data suggested that metabolic pathways, carbon metabolism, methane metabolism, biosynthesis of amino acids, glycine, serine and threonine metabolism, and pyruvate metabolism pathways were commonly identified in both transcriptome and metabolism analyses (Fig. 8A). Specifically, non-targeted metabolism analysis revealed upregulation of organic acids related to glutamate and ROS antioxidant metabolism including D-glutamine, L-glutamate and D-proline induced by KP relative to AWS in mushroom fruit bodies (Fig. 8B; Table S5).

To further decipher the reprogrammed energy metabolic pathway between KP and AWS treatments in mushroom fruiting bodies, we performed targeted metabolite analysis of 40 metabolites. This analysis revealed that 16 metabolites related to energy metabolism were significantly upregulated, while only 3 were significantly downregulated in KP-treated samples compared to AWS-treated ones in mushroom fruiting bodies (Figure S4; Table S6). Notably, glucose content increased tenfold in KP-treated samples compared to AWS-treated ones.

In conclusion, we proposed a metabolic pathway in mushroom samples treated with KP relative to AWS (Fig. 8C). KP treatment promoted the accumulation of polysaccharides, fatty acids and amino acids biosynthesis. Intermediate metabolites positively associated with these processes included L-glutamate, glucose, pyruvate, AcCoA, α-KG and D-glutamine, while some metabolites and regulatory genes, such as FDH1, AP1 and Asp were negatively correlated with these processes (Fig. 8C; Tables S3-S5).

Discussions

KP (*Caragana korshinskii* Kom.), as a drought-tolerant perennial mesquite shrub represents a significant lignocellulosic biomass resource. Cultivation of edible fungi has proven to be an efficient biological method for converting agroforestry by-products, such as KP with their abundant lignocellulosic biomass into valuable

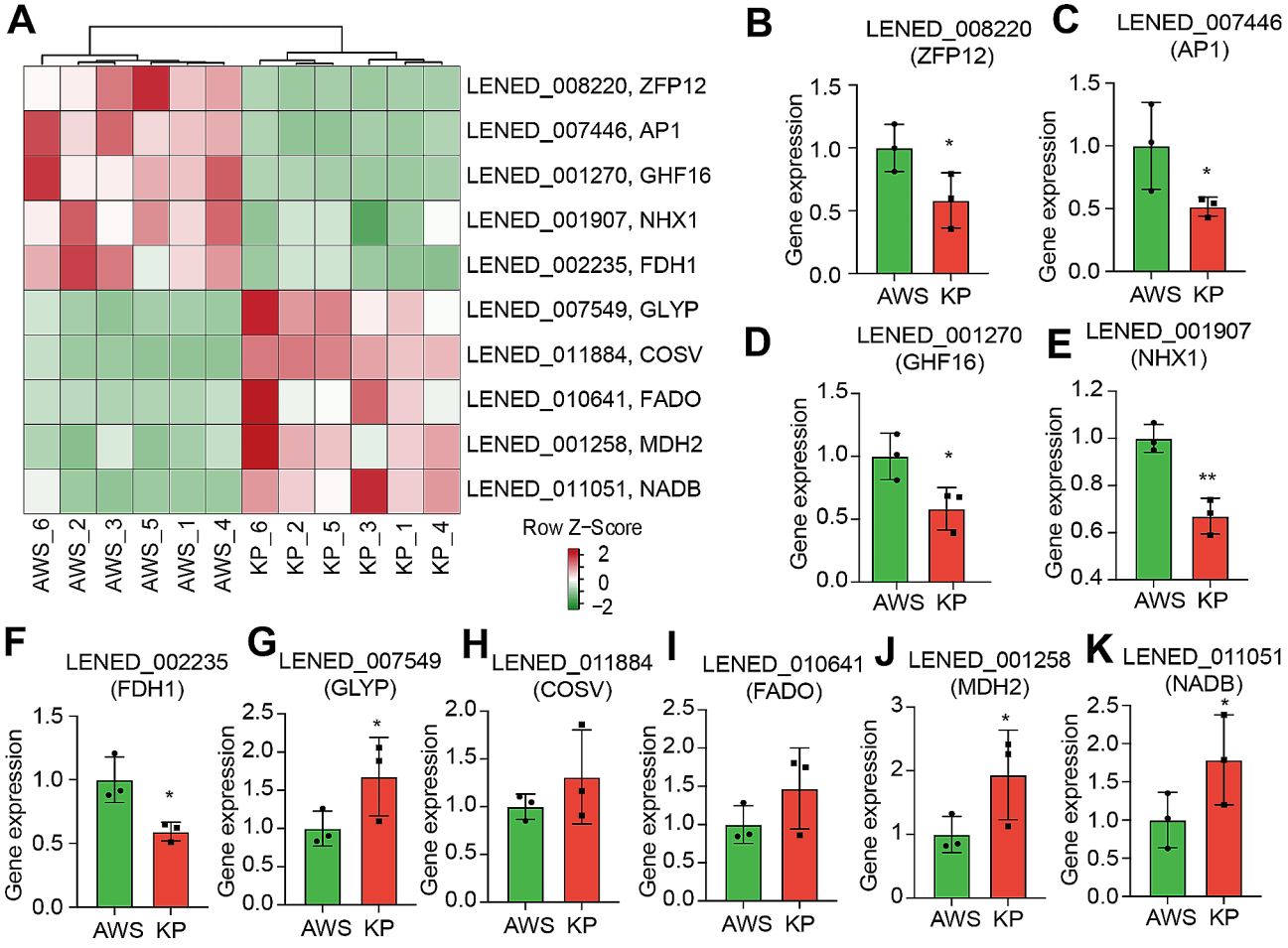

Fig. 5 Validation of top 1% differentially expressed genes in the samples of mushroom induced by AWS and KP. **A**, Heatmap representing the relative abundance of 1% DEGs based on transcriptome data. **B**-**K**, Relative expression levels of specific genes (*LENED_008220*, *LENED_007446*, *LENED_001270*, *LENED_001907*, *LENED_ 002235*, *LENED_007549*, *LENED_011884*, *LENED_010641*, *LENED_001258* and *LENED_011051*) induced by KP relative to AWS in mushroom fruiting body. Data represent means ± S.E. ($n = 3$). Symbols "*" and "**" represent the significant differences at $P < 0.05$, and $P < 0.01$, respectively, based on Student *t*-test

mushroom products. Previous studies have highlighted the important role of KP as a substrate ingredient for mushroom cultivation [10, 12, 33]. However, reports on the molecular mechanisms by which KP effects mushroom fruiting bodies have been limited. In this study, we combined transcriptome and metabolism analysis to identify key genes and biological pathways altered by KP in mushroom fruiting bodies. We here identified several genes of interest and enriched biological pathways among the top 1% DEGs and DAMs. The combined analysis reveals carbon metabolism, biosynthesis of amino acids and pyruvate metabolism pathways were commonly identified in both transcriptome and metabolism analyses. Some DEGs and DAMs related to these pathways were confirmed by qPCR and targeted metabolism approaches, respectively. These evidences suggest that reprogrammed carbon metabolism and oxidoreductase pathways act critical roles in the enhanced response of mushroom to KP substrates. This study may inform targeted genetic modifications to enhance the economic values of mushroom production.

Promoted effects of KP on mushroom nutritional features

Nutritionally, mushrooms are an excellent source of proteins, polysaccharides, dietary fibers, vitamins and minerals [34]. These nutritional features of the fruiting bodies significantly impact the commercial value and production efficiency of *L. edodes*. Different substrates can influence these attributes. Our study revealed that the fat content, polysaccharide and total sugar content in mushroom fruiting bodies were significantly enhanced by KP supplementation (Fig. 1F and S1A-B). Consistently, highlighted that the crude polysaccharide content was highest (6.12%) in *P. eryngii* mushrooms grown on a substrate containing 38% KP, a 70.47% increase compared to those grown on the control substrate (3.59%) [10]. These findings suggest that KP supplementation in

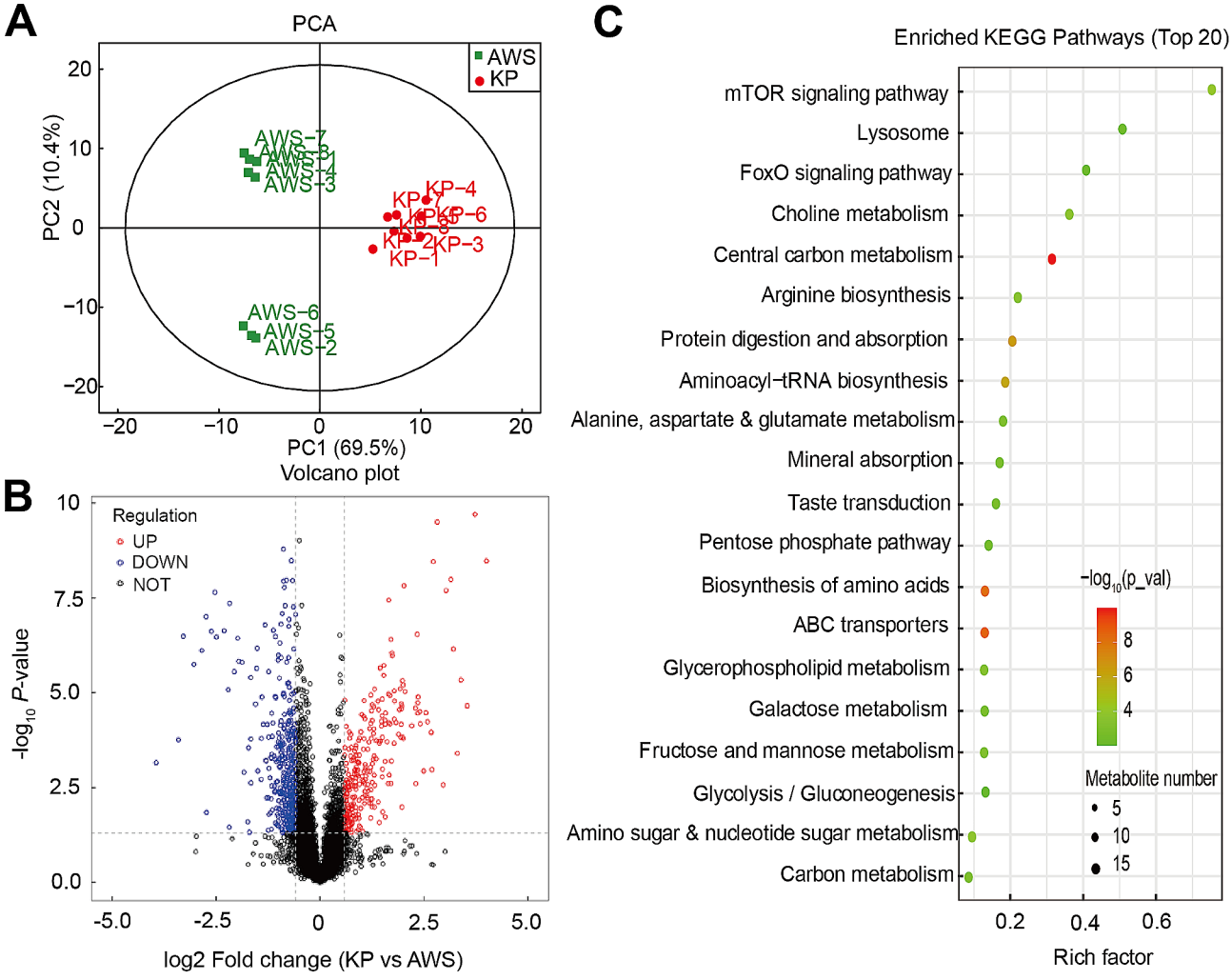

Fig. 6 Non-targeted metabolism analysis in *Lentinula edodes* samples induced by AWS and KP. **A**, Principal component analysis on non-targeted metabolism in *Lentinula edodes* samples induced by AWS and KP. **B**, Volcano plot representing differentially abundant metabolites (DAMs) in *Lentinula edodes* samples induced between AWS and KP. **C**, KEGG analysis on the list of DAMs in *Lentinula edodes* samples induced between AWS and KP

mushroom substrates can notably enhance polysaccharide accumulation.

Carbon metabolic pathways involved in KP-stimulated effects

Carbon metabolism, the citric acid cycle (TCA cycle) and oxidoreductase metabolism are central biochemical pathways in cellular energy metabolism. First, in carbon metabolism, polysaccharides are synthesized from two forms of activated glucose molecules: UDP-glucose and ADP-glucose with glucose being central to energy consumption. In this study, we propose that KP enhances polysaccharide accumulation, which is closely associated with increased levels of glucose-6-phosphate (Fig. 8B). Theoretically, numerous enzymes such as phosphoglucomutase (PGM) and UDPG-dehydrogenase (UGD) are involved in producing precursors for polysaccharide biosynthesis and are closely related to polysaccharide production [35]. In consistent with the increased levels of glucose and glucose-6-phosphate, we observed a significant increase in the relative expression of *UGD* gene (*LENED_008601*) in KP-treated mushroom fruiting bodies (Fig. 5H). Which is indicating that polysaccharide formation occurs at the branch point between the Embden-Meyerhof-Parnas (EMP) pathway and the later stages of glycogen and sugar biosynthesis [36].

Mitochondria TCA metabolism stimulated by KP

In addition, TCA cycle is central for metabolism, which provides intermediates that are utilized for the formation of energy and amino acids. Mitochondria are the primary oxygen-consuming organelles in cells, housing the oxidative phosphorylation reaction, which couples oxygen consumption by the mitochondrial respiratory chain (MRC) with the conversion of energy to the chemical form of adenosine triphosphate (ATP). Cytochrome *c* oxidase (COX),

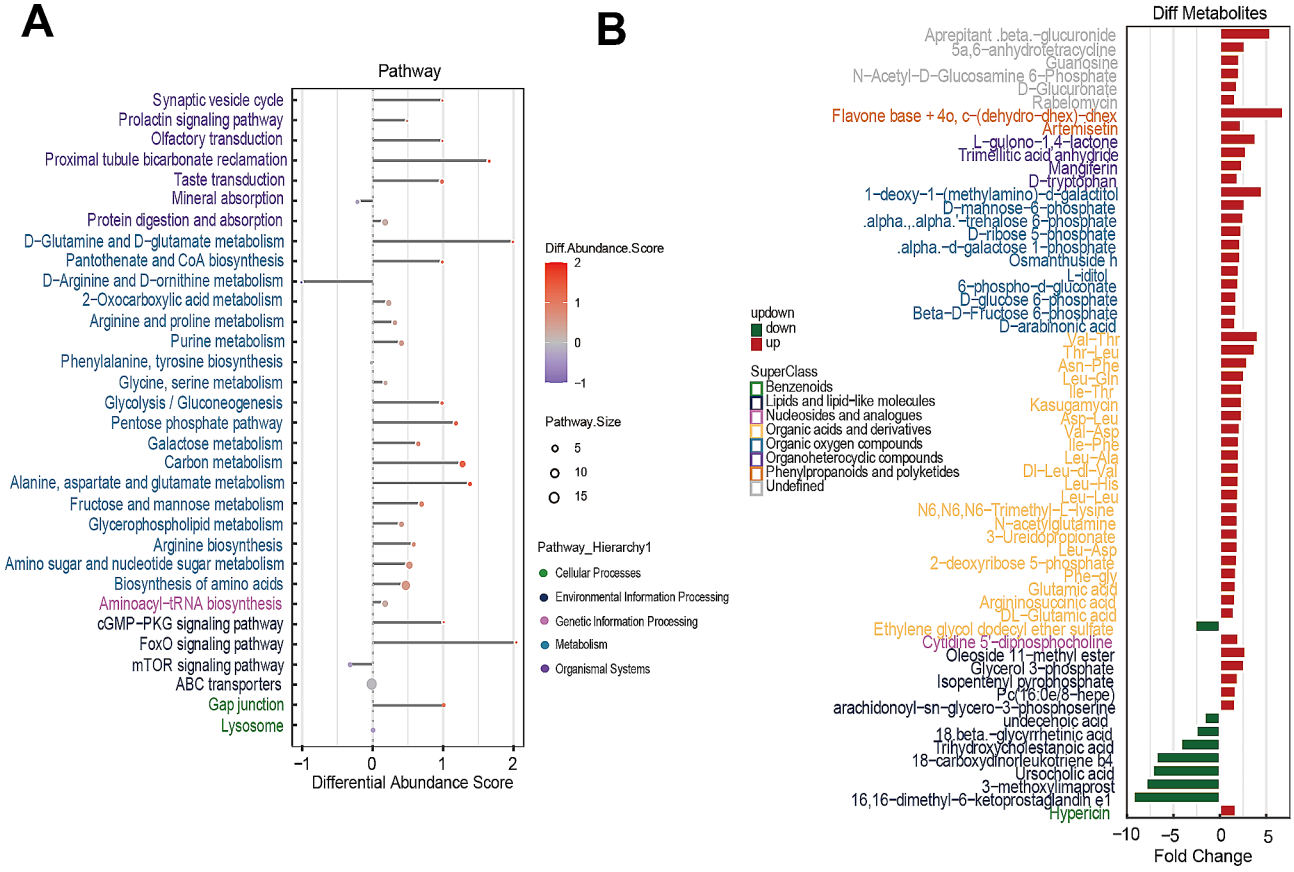

Fig. 7 Pathway enrichment analysis in differentially abundant metabolites. **A**, Regulation of enriched metabolic pathways within different hierarchies. **B**, DAMs in different super classes in mushroom fruiting body treated with KP relative to AWS

an important multiprotein enzymatic complex in the MRC is a major consumer of cellular oxygen [37]. We identified that COX expression (*LENED_011884*) was significantly enhanced by KP in mushroom fruiting bodies, potentially ensuring an adequate ATP supply for energy metabolism (Fig. 5; Table S4). The upregulation of COX expression hence could accelerate the electron transport chain leading to the complete oxidation of reactive oxygen species [38].

Cellular redox homeostasis positively associated with KP effects

Cellular redox homeostasis is essential for the maintenance of many cellular processes including oxidoreductase metabolic reaction and response to ROS. In this regard, some amino acids as protein components also participate in cellular redox homeostasis [39, 40]. In our study, we observed a significant increase in glutamine and glutamate levels in KP-induced mushroom fruiting bodies (Fig. 8B), which is in conjunction with a limited electron pool and dynamic ATP consumption, ensures energy production, e.g., via oxidative phosphorylation, by the increased activity of cytochrome *c* oxidase (*LENED_011884*) induced by KP as mentioned earlier. Thus, mushrooms can maintain a relatively stable redox state [41]. Furthermore, the increase in *malate dehydrogenase (LENED_001258)* and *GAPDH (LENED_003203)* expression induced by KP in mushroom fruiting bodies (Fig. 5; Table S4) also indicates the activation of glycolysis (Fig. 8A). This activation potentially providing additional ATP for energy metabolism [42–44]. These findings suggest that KP may help maintain stable cellular redox status and hence oxidoreductase metabolism in mushrooms by balancing glutamine metabolism, glycolysis and oxidative phosphorylation.

Exploring uncharted DEGs with potential roles

Moreover, identifying uncharted DEGs responsive to KP could provide insight into novel regulatory mechanism of mushroom quality and nutritional values. Notably, some DEGs identified in our study have been reported in previous research, including FAD-dependent oxidoreductase (*LENED_010641*), Na^+ solute symporter (*LENED_001907*), Cytochrome P450 (*LENED_006144*) [22], NAD-binding protein [11, 45] and genes related to various phases of glycolysis and the pentose phosphate pathway [11], such as glyceraldehyde-3-phosphate dehydrogenase (*LENED_003203*), phosphoglucomutase (*LENED_002022*) and glucose dehydrogenase (*LENED_001535*) (Table S4). However, the functions of most identified DEGs remain unknown or unreported. Therefore, we emphasize the need

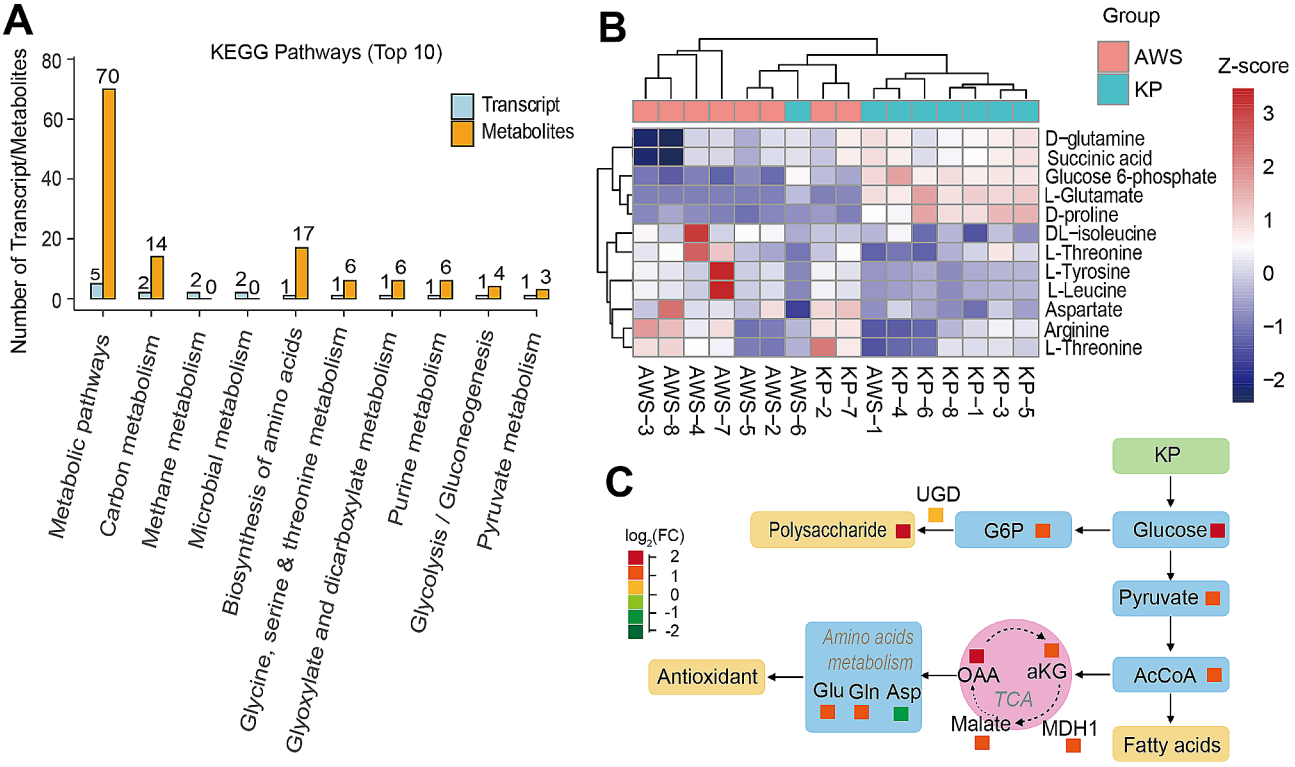

Fig. 8 Integrative analysis of transcriptome and metabolism in mushrooms treated with AWS and KP. **A**, Overlapped KEGG pathways analysis on transcriptome and metabolism. **B**, Heatmap representing the DAMs related to organic acids in the antioxidant scavenging process using targeted metabolism between AWS and KP. **C**, Summarized metabolic pathway in *Lentinula edodes* samples regulated by KP, relative to AWS

for further functional genomics studies on mushrooms to advance molecular breeding efforts for more precisely targeted economic traits.

Supplementary Information

The online version contains supplementary material available at https://doi.org/10.1186/s12864-024-10666-8.

Supplementary Material 1

Supplementary Material 2

Acknowledgements
We especially thank Dr. Yaozong Wu (Shanghai Honest Biotechnology, Ltd, China) and Zhongkang omics Biotech Company for their contributions to the technical guidance and support concerning the LC-MS/MS analysis in the study.

Author contributions
YZ ideated and designed the experiments. YY, HL, ZH and XM conducted the experiments and analyzed the data, YZ drafted the manuscript. YZ and ZH revised the manuscript. All authors have contributed to, approved the manuscript.

Funding
This work was supported by Science and Technology Achievement Transformation Project of Qinghai Province (Grant nos. 2023-NK-140), Science and Technology Commissioner Project of Qinghai Province (Grant nos. 2024-NK-P05) and Qinghai Province "Kunlun Talents · High-end innovative and entrepreneurial talents" project.

Data availability
All related sequencing data are deposited in NCBI Sequence Read Archive (SRA) database. The link to access the data is: https://www.ncbi.nlm.nih.gov/sra?term=PRJNA1108197. The bioProject accession is PRJNA1108197.

Declarations

Ethics approval and consent to participate
Our fruit tree collection work complies with the laws of the People's Republic of China and has a permission letter from Academy of Agriculture and Forestry, Qinghai University. The study complied with relevant institutional, national, and international guidelines and legislation.

Consent for publication
Not applicable.

Competing interests
The authors declare no competing interests.

Author details
[1]Qinghai University, Xining 810016, China
[2]College of Ecol-Environmental Engineering, Qinghai University, Xining 810016, China
[3]Academy of Agriculture and Forestry, Qinghai University, Xining 810016, China
[4]Qinghai Key Laboratory of Genetic Breeding of Highland Barley/Qinghai Highland Barley Sub- Center of National Wheat Improvement Center, Xining 810016, China
[5]Laboratory for Research and Utilization of Qinghai Tibet Plateau Germplasm Resources, Xining 810016, China

Received: 6 March 2024 / Accepted: 25 July 2024
Published online: 06 August 2024

References

1. Cheng X, Huang M, Si BC, Yu M, Shao M. The differences of water balance components of Caragana Korshinkii grown in homogeneous and layered soils in the desert–Loess Plateau transition zone. J arid Environ. 2013;11(98):10–9.
2. Huang H, Zhang Y. Growth suitability of Caragana Korshinkii in three water types afforested area in northern mountain of Lanzhou City. Sci Soil Water Conserv. 2013;2(11):72–6.
3. Mo B, Cai G, Lu J, Wang Z, Wang D, Qi J, Yang L, Dang H. Soil water use and balance characteristics in mature forest land profile of Caragana korshinskii in Semiarid Loess Area. Ying Yong Sheng Tai Xue bao. 2013;33(13):4011–20.
4. Guo Z, Shao M. Effect of artificial Caragana korshinskii forest on soil water in the semiarid area of Loess hilly region. Scientia Silvae Sinicae. 2010;46(12):1–7.
5. Manavalan T, Manavalan A, Heese K. Characterization of lignocellulolytic enzymes from white-rot fungi. Curr Microbiol. 2015;70:485–98.
6. Montoya S, Sánchez ÓJ, Levin L. Production of lignocellulolytic enzymes from three white-rot fungi by solid-state fermentation and mathematical modeling. Afr J Biotechnol. 2015;14(15):1304–17.
7. Chang ST. Overview of mushroom cultivation and utilization as functional foods. John *Wiley Sons, Ltd. New York, pp. 2008. 281 – 234*.
8. Sánchez C. Lignocellulosic residues: biodegradation and bioconversion by fungi. Biotechnol Adv. 2009;27(2):185–94.
9. Sun F, Xing Z. Research on advantage and new use of Korshinsk Peashrub resources. Agri Sci Technol. 2014;15(4):709.
10. Zou Y, Du F, Zhang H, Hu Q. Evaluation of Korshinsk Peashrub (Caragana korshinskii Kom.) As a substrate for the cultivation of Pleurotus Eryngii. Waste Biomass Valor. 2019;10:2879–85.
11. Yang C, Ma L, Xiao D, Liu X, Jiang X, Lin Y. Comparative transcriptomics reveals unique pine wood decay strategies in the Sparassis latifolia. Sci Rep. 2022;12(1):19875.
12. Du F, Qu J, Hu Q, Yuan X, Yin G, Wang L, Zou Y. Maximizing the value of Korshinsk peashrub branches by the integration of Pleurotus tuoliensis cultivation and anaerobic digestion of spent mushroom substrate. Renew Energy. 2021;179:679–86.
13. Zhang J, Ren A, Chen H, Zhao M, Shi L, Chen M, Wang H, Feng Z. Transcriptome analysis and its application in identifying genes associated with fruiting body development in basidiomycete Hypsizygus Marmoreus. PLoS ONE. 2015;10(4):e0123025.
14. Lee HJ, Suh DH, Jung ES, Park HM, Jung G-Y, Do S-G, Lee CH. Metabolomics of Lonicera caerulea fruit during ripening and its relationship with color and antioxidant activity. Food Res Int. 2015;78:343–51.
15. Jang YK, Jung ES, Lee H-A, Choi D, Lee CH. Metabolomic characterization of hot pepper (Capsicum annuum CM334) during fruit development. J agri food chem. 2015;63(43):9452–60.
16. Harada A, Yoneyama S, Doi S, Aoyama M. Changes in contents of free amino acids and soluble carbohydrates during fruit-body development of Hypsizygus marmoreus. Food chem. 2003;83(3):343–7.
17. Gao W, Sun H-X, Xiao H, Cui G, Hillwig ML, Jackson A, Wang X, Shen Y, Zhao N, Zhang L. Combining metabolomics and transcriptomics to characterize tanshinone biosynthesis in Salvia miltiorrhiza. BMC Genom. 2014;15:1–14.
18. Kim HY, Heo DY, Park HM, Singh D, Lee CH. Metabolomic and transcriptomic comparison of solid-state and submerged fermentation of Penicillium Expansum KACC 40815. PLoS ONE. 2016;11(2):e0149012.
19. Huang H, Yao Q, Xia E, Gao L. Metabolomics and transcriptomics analyses reveal nitrogen influences on the accumulation of flavonoids and amino acids in young shoots of tea plant (Camellia sinensis L.) associated with tea flavor. J agri food chem. 2018;66(37):9828–38.
20. Song H-Y, Kim D-H, Kim J-M. Comparative transcriptome analysis of dikaryotic mycelia and mature fruiting bodies in the edible mushroom Lentinula edodes. Sci rep. 2018;8(1):8983.
21. Wang Y, Zeng X, Liu W. De novo transcriptomic analysis during Lentinula edodes fruiting body growth. Gene. 2018;641:326–34.
22. Yan D, Gao Q, Rong C, Liu Y, Song S, Yu Q, Zhou K, Liao Y. Comparative transcriptome analysis of abnormal cap and healthy fruiting bodies of the edible mushroom Lentinula edodes. Fungal Genet Biol. 2021;156:103614.
23. Sambucetti M, Zuleta A. Resistant starch in dietary fiber values measured by the AOAC method in different cereals. Cereal Chem. 1996;73(6):759–61.
24. Thiex N. Evaluation of analytical methods for the determination of moisture, crude protein, crude fat, and crude fiber in distillers dried grains with solubles. J AOAC int. 2009;92(1):61–73.
25. Fu X, Zhou X, Deng B, Shang X, Fang S. Seasonal and genotypic variation of water-soluble polysaccharide content in leaves of Cyclocarya paliurus. South for. 2015;77(3):231–6.
26. McCready R, Guggolz J, Siliviera V, Owens H. Biochemical methods. Anal Chem. 1950;22:1156.
27. Jiang C, Bi Y, Mo J, Zhang R, Qu M, Feng S, Essemine J. Proteome and transcriptome reveal the involvement of heat shock proteins and antioxidant system in thermotolerance of Clematis florida. Sci Rep. 2020;10(1):8883.
28. Dobin A, Davis CA, Schlesinger F, Drenkow J, Zaleski C, Jha S, Batut P, Chaisson M, Gingeras TR. STAR: ultrafast universal RNA-seq aligner. Bioinformatics. 2013;29(1):15–21.
29. Chen F, Zheng G, Qu M, Wang Y, Lyu M-JA, Zhu X-G. Knocking out NEGATIVE REGULATOR OF PHOTOSYNTHESIS 1 increases rice leaf photosynthesis and biomass production in the field. J Exp Bot. 2021;72(5):1836–49.
30. Hamdani S, Wang H, Zheng G, Perveen S, Qu M, Khan N, Khan W, Jiang J, Li M, Liu X. Genome-wide association study identifies variation of glucosidase being linked to natural variation of the maximal quantum yield of photosystem II. Physiol Plant. 2019;166(1):105–19.
31. Qu M, Chen G, Bunce JA, Zhu X, Sicher RC. Systematic biology analysis on photosynthetic carbon metabolism of maize leaf following sudden heat shock under elevated CO2. Sci Rep. 2018;8(1):7849.
32. Li J, Essemine J, Shang C, Zhang H, Zhu X, Yu J, Chen G, Qu M, Sun D. Combined proteomics and metabolism analysis unravels prominent roles of antioxidant system in the prevention of alfalfa (Medicago sativa L.) against salt stress. Int J Mol Sci. 2020;21(3):909.
33. Yang Y, Li C, Nie J, Xing H, Li Z, Wang Z. Study on substrate formula including Korshinsk peashrub and corncobs for Pleurotus ostreatus cultivation. Edible Fungi. 2011;4:20–2.
34. Politowicz J, Lech K, Lipan L, Figiel A, Carbonell-Barrachina ÁA. Volatile composition and sensory profile of shiitake mushrooms as affected by drying method. J Sci Food Agri. 2018;98(4):1511–21.
35. Zhu Z-Y, Liu X-C, Dong F-Y, Guo M-Z, Wang X-T, Wang Z, Zhang Y-M. Influence of fermentation conditions on polysaccharide production and the activities of enzymes involved in the polysaccharide synthesis of Cordyceps Militaris. Appl Microbiol Biotechnol. 2016;100:3909–21.
36. Tang Y-J, Zhong J-J. Exopolysaccharide biosynthesis and related enzyme activities of the medicinal fungus, Ganoderma Lucidum, grown on lactose in a bioreactor. Biotechnol lett. 2002;24:1023–6.
37. Degn H, Wohlrab H. Measurement of steady-state values of respiration rate and oxidation levels of respiratory pigments at low oxygen tensions. A new technique. Biochim Biophys Acta. 1971;245(2):347–55.
38. Lin Y, Lin H, Chen Y, Wang H, Lin M, Ritenour MA, Lin Y. The role of ROS-induced change of respiratory metabolism in pulp breakdown development of longan fruit during storage. Food chem. 2020;305:125439.
39. Han M, Xu M, Su T, Wang S, Wu L, Feng J, Ding C. Transcriptome analysis reveals critical genes and pathways in carbon metabolism and ribosome biogenesis in poplar fertilized with glutamine. Int J Mol Sci. 2022;23(17):9998.
40. Lee YH, Foster J, Chen J, Voll LM, Weber AP, Tegeder M. AAP1 transports uncharged amino acids into roots of Arabidopsis. Plant J. 2007;50(2):305–19.
41. Baier M, Dietz K-J. Chloroplasts as source and target of cellular redox regulation: a discussion on chloroplast redox signals in the context of plant physiology. J exp bot. 2005;56(416):1449–62.
42. Chen X, Yang B, Huang W, Wang T, Li Y, Zhong Z, Yang L, Li S, Tian J. Comparative proteomic analysis reveals elevated capacity for photosynthesis in polyphenol oxidase expression-silenced Clematis terniflora DC. Leaves. Int J Mol Sci. 2018;19(12):3897.
43. Zhao Z, Assmann SM. The glycolytic enzyme, phosphoglycerate mutase, has critical roles in stomatal movement, vegetative growth, and pollen production in Arabidopsis thaliana. J exp bot. 2011;62(14):5179–89.
44. Rosa-Téllez S, Anoman AD, Flores-Tornero M, Toujani W, Alseek S, Fernie AR, Nebauer SG, Muñoz-Bertomeu J, Segura J, Ros R. Phosphoglycerate kinases are co-regulated to adjust metabolism and to optimize growth. Plant Physiol. 2018;176(2):1182–98.
45. Kim JY, Kim DY, Park Y-J, Jang M-J. Transcriptome analysis of the edible mushroom Lentinula edodes in response to blue light. PLoS ONE. 2020;15(3):e0230680.

Publisher's Note